

Investigation of the Effect of Debris-Induced Damage for Constructing Tsunami Fragility Curves for Buildings

J. Macabuag¹, T. Rossetto², I. Ioannou³

¹EngD Candidate, University College London, UK

²Professor, University College London, UK

³Post-doctoral researcher, University College London, UK

ABSTRACT

Tsunami fragility curves are statistical models which form a key component of tsunami risk models, as they provide a probabilistic link between a Tsunami Intensity Measure (TIM) and building damage. Building damage due to tsunamis can occur due to fluid effects (e.g. drag) and debris impact, two effects which have different implications for building damage levels and mechanisms. However, existing studies often pool all available damage data for a location regardless of whether damage was caused by fluid or debris effects, and so it is not clear whether the inclusion of debris-induced damage introduces bias in existing fragility curves. This paper uses a detailed disaggregated damage dataset from the 2011 Great East Japan Earthquake and Tsunami together with several advanced statistical methods in order to identify the effect that debris-induced damage has on fragility function derivation.

Buildings are identified which are most likely to have sustained significant debris damage, based on the proportion of nearby buildings which have been designated as “washed away” in their post-tsunami survey. Fragility curves are then constructed for observed inundation depth and simulated force, and fragility curves with/without debris impact are compared for each damage state. Finally complex models which include all buildings and additional parameters corresponding to debris impact are considered. The influence of debris model parameters on determining building damage was shown to be significant for all but the lowest damage state (“minor damage”), and more complex fragility functions which incorporate debris model parameters were shown to have a statistically significant better fit to the observed damage data than models which omitted debris information.

Keywords: Tsunami damage; Empirical fragility curves; Generalised linear models; Generalised additive models; Ordinary Least Squares; Cross-validation; Bootstrap techniques; Multiple imputation; Intensity measures; Inundation simulation; Great East Japan Earthquake and Tsunami 2011; Debris.

ACKNOWLEDGEMENTS

The first author was funded by EPSRC Engineering Doctorate Programme and the Willis Research Network, and travel to conduct this collaborative work was kindly funded by the Sasakawa Foundation and the Earthquake Engineering Field Investigation Team travel grant. Co-author Ioanna Ioannou was funded by the

¹ Corresponding Author: J. Macabuag, University College London, joshua.macabuag.12@ucl.ac.uk

EPSRC Challenging Risk grant. We would like to thank Prof Richard Chandler of the Department of Statistical Science, UCL, for advising on the statistical analysis conducted in this study. We would also like to acknowledge the many years of successful collaboration between EPICentre, UCL (UK) and IRIDeS, Tohoku University (Japan) which has made this work possible.

INTRODUCTION

Tsunami fragility curves for buildings provide a probabilistic link between a Tsunami Intensity Measure (TIM) and building damage. They are a component of tsunami risk models, and so are vital for land-use and emergency planning, as well as human and financial loss estimation.

Compared to seismic studies, few fragility functions for buildings affected by tsunami exist, and the vast majority have been based solely on empirical data (post-tsunami building damage surveys). Empirical fragility curves are very specific to the building type and flow conditions from where the data was taken (Suppasri, Charvet, Kentaro, & Imamura, 2014), and so should ideally not be generalized or applied to different geographical locations. However, given the scarcity of high-quality tsunami damage data, empirical fragility functions are necessarily often applied to different locations and conditions from where they were derived, and in such cases it is necessary to understand how fragility functions may be adapted to the new conditions.

Tsunami-induced building damage can arise due to fluid forces (hydrostatic and hydrodynamic) and debris effects (impact and damming). Various TIMs have been used in recent fragility studies to describe flow conditions, such as depth, velocity and hydrodynamic force (Koshimura et al. 2009, Charvet et al. 2014, Tanaka and Kondo 2015). Macabuag et al., (2016) present a methodology for selecting the optimum TIM for a given dataset, however, TIMs in existing fragility studies rarely specifically describe debris-induced damage.

Charvet, Suppasri, Kimura, Sugawara, & Imamura (2014) generate fragility functions considering that debris is mostly composed of the remains of collapsed buildings, and as such designates buildings as having been affected by debris if they are within a given distance (distances from 10m to 150m are tried) of a building that has been washed away. However, this method does not make any allowance for the size of collapsed buildings or the number of collapsed buildings (i.e. one small collapsed structure, has the same effect as several large collapsed structures).

This paper presents a preliminary investigation to address the following research questions:

1. How does the presence of debris in tsunami inland flow affect fragility functions?
2. Is it possible to quantify this effect by separating fluid and debris-induced damage in fragility function derivation?

In this paper a preliminary methodology for quantifying debris-related effects on fragility functions is presented. Detailed, disaggregated building-by-building damage data from the 2011 Great East Japan Earthquake (GEJE) is used to develop tsunami fragility curves for buildings in Japan considering the effect of debris in the flow. Note that the definition of debris impact is beyond the scope of this paper, and the focus is to instead demonstrate whether it is feasible to identify debris impact, and to highlight what affect this might have on fragility functions. An important application of the future development of this work will be to define how fragility curves could be adjusted to account for locations of increased likelihood of debris (e.g. downstream of ports or areas of lightly constructed buildings likely to collapse in tsunami flow) for both the engineering and insurance industries.

PRESENTATION OF DATA AND ANALYTICAL MODEL

Building Damage Dataset

The building damage data used in this paper is taken from the GEJE (2011) building damage database compiled by Japan's Ministry of Land Infrastructure Tourism and Transport (MLIT). The database is

comprised of relevant information (including observed inundation depth and damage state (Table 1)) for each individual building located within the inundation area of the 2011 GEJE.

This paper considers the same dataset as Macabuag et al. (2016), which comprised of three case-study locations, namely the towns of Ishinokami, Kesenuma and Onagawa, which represent 80%, 15%, and 5%, respectively of the combined dataset. It is noted that as DS5 and DS6 do not represent progressively worse damage states they will be combined (into DS5*) for the purposes of fragility function derivation.

Damage State		Description	Use
DS0	No Damage	Water does not enter into the building footprint	Immediate occupancy
DS1	Minor Damage	Water enters below the ground floor	Possible to use immediately after minor floor and wall cleanup
DS2	Moderate Damage	Water inundates to less than 1m above the ground floor	Possible to use after moderate repairs
DS3	Major Damage	Water inundates to more than 1m above the floor (but below the ceiling)	Possible to use after major repairs
DS4	Complete Damage	The building is inundated above the ground floor level	Major work is required for re-use of the building
DS5	DS5*	Collapsed	Structural elements are significantly damaged
DS6		Washed Away	The building is completely washed away except for the foundation

Table 1: Damage state definitions used by the Japanese Ministry of Land Infrastructure Tourism and Transport following the 2011 Great East Japan Earthquake and Tsunami. Descriptions from Japan Cabinet Office (2013), usage descriptions are after Suppasri et al. (2014).

The construction material of a building has been shown to significantly affect its building damage probability (Suppasri et al. 2012a). Macabuag et al., (2016) shows that for this dataset the damage state distributions and fragility curves for reinforced concrete (RC) and steel construction materials are very similar to each other, and so may be grouped together and analysed simultaneously (termed as “engineered” buildings for the remainder of this paper). Conversely, fragility curves for engineered and non-engineered (wood and masonry) buildings differ in both slopes and intercepts, and so it is appropriate to consider these material groups separately. Hence, in this paper fragility curves are developed specifically for the engineered material class (4570 buildings), in order to account for building material whilst maintaining large enough datasets to avoid significantly increasing uncertainty in the model parameter estimates.

Buildings of unknown construction material make up 18.1% of the total dataset within the inundated area, representing a significant proportion of the data. Previous studies (e.g. Suppasri et al. 2013) generally conduct complete-case analysis (i.e. they remove any partial data, such as buildings of unknown material, from their fragility analysis). However, Macabuag et al. (2016) showed that missing data can only be removed if it can be shown to be Missing Completely At Random (where the data is missing purely by chance so that there is no relationship between the buildings that have missing material data and other attributes such as the building height, size and use) and that this is not the case for the 2011 MLIT Japan data. Multiple Imputation (MI) (which involves replacing missing observed data with substituted values estimated multiple times via stochastic regression models built on the other attributes) has been shown to be an acceptable method for estimating missing data, and so is conducted in order to estimate building material based on footprint area, damage state, building use, and observed inundation depth used to complete the data.

Tsunami Inundation Simulation Data

To supplement the observed inundation depth data, a numerical inundation simulation is conducted for the case-study locations to calculate simulated peak inundation depth, velocity, Froude number (a measure of velocity non-dimensionalised by depth) and momentum flux (a product of depth and velocity, proportional to hydrodynamic drag force). Macabuag et al. (2016) propose a methodology for comparing multiple TIMs and

concludes that for this dataset an equivalent quasi-steady force proposed by Qi et al. (2014) (and suggested by Lloyd (2014) to represent the force of a tsunami inundation on buildings) is the TIM which shows the optimal fit to observed damage data. It is evaluated via two different flow regimes determined by Froude Number, and it relates h , v and blockage ratio (building width/channel width, which is taken as 25% in this study) to force, denoted here as F_{QS} . Readers are referred to Qi et al. (2014) for the calculation procedure. The two TIMs that are considered in this paper are therefore observed inundation depth (h_{obs}) and the simulated equivalent quasi-steady force (F_{QS}).

The numerical tsunami inundation model is presented in detail and validated by Adriano and Koshimura (2016). The tsunami source model used in this study is the time-dependent slip propagation model presented in Satake et al. (2013). The wave propagation and inundation calculation solves discretized non-linear shallow-water equations (Imamura et al. 1995; Suppasri et al. 2012) over six computational domains in a nested grid system. The non-linear shallow-water equation includes the effects of flow resistance, which is parameterised using uniform value of the Manning's roughness coefficient ($n=0.025$). The example results shown in Figure 1 are the peak values for each grid square over the simulation period.

Statistical Model

According to the GEM methodology (Rossetto et al. 2014), a statistical model suitable for the available data should be constructed. Statistical models are used to construct a relationship between building damage and the TIM, which accounts for the uncertainty in damage prediction. The statistical models can be parametric (e.g. Generalised Linear Models (GLMs), Cumulative Link Models (CLMs), or linear models with Ordinary Least Squares (OLS) parameter estimation), semi-parametric (e.g. Generalised Additive Models, GAMs) or non-parametric (e.g. kernel smoothers).

Macabuag et al. (2016) presents three stages of analysis conducted in order to identify suitable statistical models for representing the imputed dataset: first a comparison of ordered and partially-ordered cumulative link models, then a sensitivity analysis of data aggregation and parameter estimation techniques, finally a sensitivity analysis of semi-parametric model parameters. Following this analysis OLS parameter estimation is quantitatively shown to be unsuitable for fragility function estimation as it suffers from the issues of data aggregation and violates several linear model assumptions, semi-parametric models are not recommended for prediction purposes, and partially ordered models are shown to demonstrate a significantly better fit to this dataset than ordered models.

Therefore partially-ordered probit models are selected for this study where fragility curves corresponding to the five damage states (DS1-DS5*) are determined by assigning a damage response indicator, ds , to each building, which is considered to follow a multinomial distribution. Each building is also assigned a TIM value, x_j . The designation of this debris variable is discussed in detail below. The main advantage of this model over separate GLMs fitted to binary data, is its ability to use all available information regarding the data in the database, it recognises that the damage is an ordinal categorical variable and accounts for the main conclusions of the exploratory analysis (Charvet et al 2014a). A probit link function is used (the inverse standard cumulative normal distribution). The model equation is given in (1) where β_0 and β_1 are the unknown regression parameters (the intercept and slope, respectively) estimated by a maximum likelihood optimisation algorithm. Uncertainty is quantified using bootstrap methods employed by Charvet et al. (2014) based on 1,000 iterations.

$$\begin{aligned}
& ds = \{0,1,2,3,4,5^*\}, \quad ds|x_j \sim \text{Multinomial} \left(P(ds = DS_i | TIM = x_j) \right) \\
\text{Random Component} \quad \text{Where,} \quad & P(ds = DS_i | TIM = x_j) = \begin{cases} 1 - P(ds \geq DS_i | x_j) \\ P(ds \geq DS_i | x_j) - P(ds \geq DS_{i+1} | x_j) \\ P(ds \geq DS_i | x_j) \end{cases} \\
& \begin{aligned} & i = 0 \\ & 0 < i < N_{DS} \\ & i = N_{DS} \end{aligned} \tag{1} \\
\text{Systematic Component} \quad & \text{and } \text{probit} \left(P(ds \geq DS_i | TIM = x_j) \right) = \beta_{0,i} + \beta_{1,i} x_{j,k} \\
\text{Parameter Estimation} \quad & \text{and } \beta_{0,i}, \beta_{1,i} \text{ estimated via Maximum Likelihood}
\end{aligned}$$

This study utilizes several “goodness of fit” tests in order to assess how well a statistical model fits the damage data, to quantitatively compare models, and to choose the model with the best fit. The coefficient of determination (R^2) denotes the proportion of the variance in the dependent variable that is predictable from the independent variable and is used in many existing studies (Gokon, Koshimura, & Matsuoka (2010); Suppasri et al. (2011)). However, R^2 does not indicate whether the most appropriate set of explanatory variables has been chosen, the correct regression methodology was used, or if there is collinearity present in the data on the explanatory variables.

Guidelines set out by Rossetto et al. (2014) recommend the use of the Likelihood Ratio Test (LRT) to compare nested models, as conducted by some recent studies (I. Charvet, Ioannou, Rossetto, a. Suppasri & Imamura 2014; Muhari et al. 2015). The likelihood statistic of a model describes the likelihood of observing the observations on which the model was fit, given the error distribution defined by that model. A more complex statistical model (one with more explanatory variables) will always fit the data on which it was fit, as well or better than a simpler model fit to the same data. The LRT tests whether the improvement in fit of a more complex model is statistically significant. The test utilizes the likelihood ratio test statistic (D) of two nested models, which is a function of the ratio of the models’ likelihood statistics (2).

$$D = -2 \log \frac{L_{\text{simple model}}}{L_{\text{complex model}}} \tag{2}$$

The distribution of the test statistic D is approximately a χ^2 distribution, with degrees of freedom equal to the difference between the degrees of freedom of the two models being tested ($df_{\text{simple model}} - df_{\text{complex model}}$). By assuming this χ^2 distribution, the probability (or p-value) of D can be computed, with a p-value < 0.05 indicating a greater than 5% chance that the difference in deviance statistics D was developed from random chance, and so the more complex model can be rejected. The likelihood ratio test will be used in this study to compare nested models.

INCORPORATION OF DEBRIS EFFECTS IN FRAGILITY FUNCTION DERIVATION

This section investigates to what extent the presence of debris in tsunami inland flow affects fragility function derivation. Buildings which are thought to have been damaged by debris effects are removed from the dataset and fragility functions are formed based only on buildings for which debris was less likely to be the main factor in defining building damage.

Method of Debris Designation

A major source of large debris within tsunami inland flow is from collapsed buildings (Charvet, Suppasri, et al., 2014), therefore buildings close to other collapsed buildings will be removed from the dataset. A regular grid of 500m is applied to each case study location, the total footprint area of all “washed away” (DS6) buildings is calculated for each grid, and if this area exceeds a threshold proportion of the total building

footprint area for that grid all buildings of that grid are deemed to have been affected by debris and so removed from the dataset. Threshold proportions (washed away area/total area) of 20%, 35% and 50% are tried.

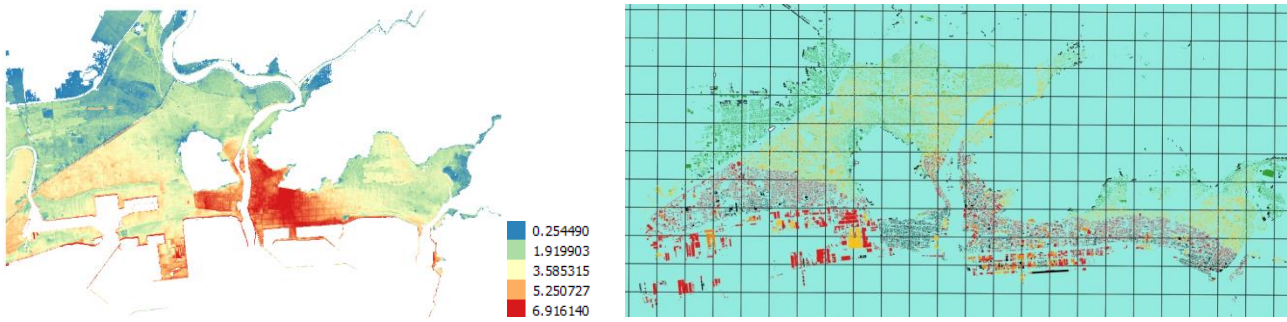


Figure 1: Plan views of Ishinomaki, Japan showing simulation results for inundation depth (left) and the 500m grid used for debris analysis (right) with buildings shown coloured according to their damage state (from DS1, green, to DS5, red, with washed away buildings denoted in black).

Exploratory Analysis of Debris Dataset

Table 2 shows the proportions of the dataset remaining after debris-affected buildings have been removed, according to each of the collapse area thresholds. It can be seen that the lowest collapse area threshold (of 20%) leads to the greatest number of buildings being removed from the dataset. Figure 2 shows histograms for all engineered buildings and for buildings not affected by debris (according to the 20% threshold), showing that buildings affected by debris fall into higher DS categories and at higher TIM values.

Threshold ($= \frac{\text{Footprint area of 'washed away' buildings within gridsquare}}{\text{Total area of all buildings in gridsquare}}$)	Number of buildings deemed to <u>not</u> be affected by debris	% of total dataset unaffected by debris
No buildings removed from dataset	4570	100%
50% of total grid building area	3982	87.1%
35% of total grid building area	3792	83.0%
20% of total grid building area	3130	68.5%

Table 2: proportions of data designated as debris-affected under various collapse area thresholds.

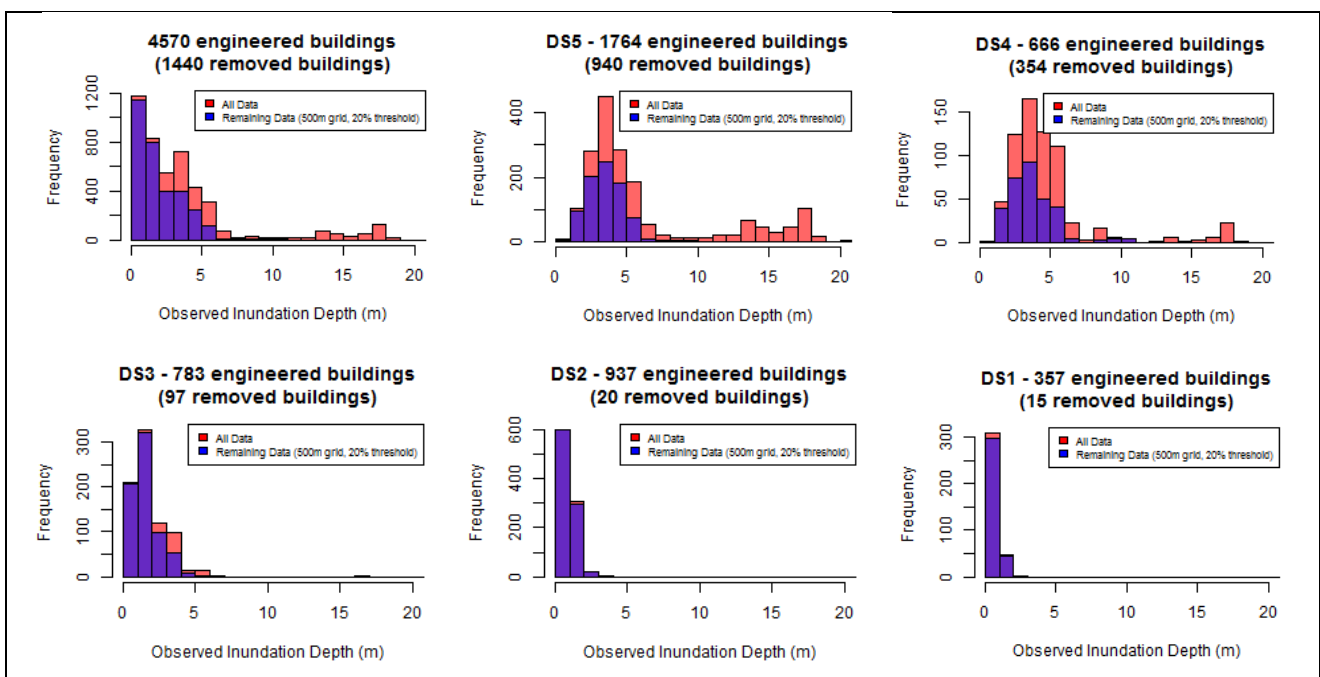


Figure 2: Histograms of observed inundation depth for engineered buildings for each DS. Distributions are shown for all engineered buildings (red) and for buildings deemed not to be affected by debris (blue, based on a 500m grid and 20% collapse area threshold).

Debris Removal Results

Figure 3 compares fragility functions formed for all engineered buildings and for those designated as unaffected by debris, for collapse area thresholds of 50%, 35% and 20%. Deviation from the fragility functions formed for all engineered buildings increases with lower threshold values (i.e. the greatest difference is seen for functions formed on data for the 20% collapse area threshold). The fragility functions for all engineered buildings and for the 20% area threshold are therefore also shown in link function (probit) space in Figure 4, and the model parameters for the inundation depth fragility functions are given in Table 3.

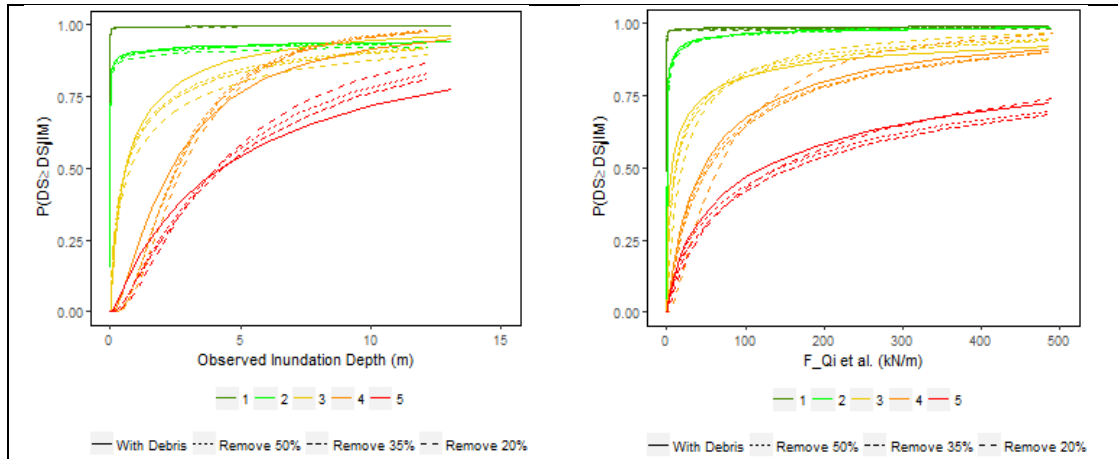


Figure 3: Fragility functions for engineered buildings with/without data removed (based on collapse area thresholds of 20%, 35% and 50%).

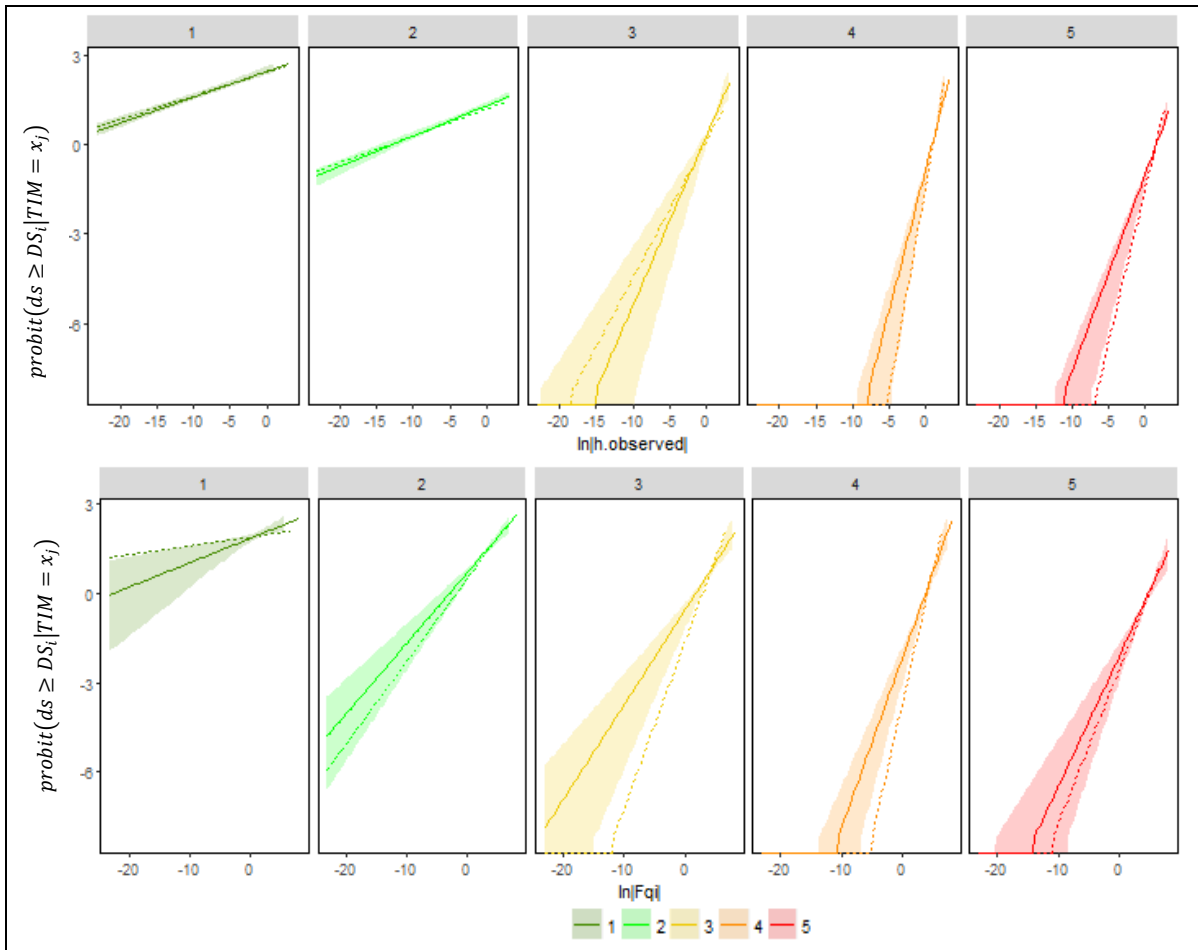


Figure 4: Link functions for observed inundation depth (top) and simulated force (bottom) for fragility functions derived for all engineered buildings (solid line, with 95% bootstrap confidence intervals) and buildings not affected by debris (for the 20% collapse area threshold).

		No Debris removal	50% threshold	35% threshold	20% threshold
β_0	0 1.(Intercept)	2.47	2.49	2.49	2.44
	1 2.(Intercept)	1.32	1.29	1.28	1.20
	2 3.(Intercept)	0.29	0.26	0.24	0.11
	3 4.(Intercept)	-0.80	-1.20	-1.21	-1.41
	4 5.(Intercept)	-0.95	-1.23	-1.25	-1.45
β_1	0 1 . $\ln h_{obs} $	0.09	0.09	0.08	0.08
	1 2 . $\ln h_{obs} $	0.10	0.10	0.10	0.09
	2 3 . $\ln h_{obs} $	0.57	0.47	0.45	0.46
	3 4 . $\ln h_{obs} $	0.95	1.30	1.28	1.38
	4 5 . $\ln h_{obs} $	0.66	0.87	0.85	1.03

Table 3: Changes in model parameters for observed inundation depth (model (1)). Green colour scale indicates decreasing values, red colour scale indicates increasing values.

The above figures show the trend that where buildings affected by debris are removed from the dataset, for higher damage states (DS4 and DS5*) the probability of damage exceedance is reduced for lower TIM values, but increased for higher TIM values. As more buildings are removed from the dataset (i.e. as the collapse area threshold decreases) the curve becomes steeper, accentuating the effect of reduced damage exceedance probabilities at lower TIM values but higher probabilities at higher TIM values (Figure 3). The opposite is true for lower damage states.

Intuitively, lower damage exceedance probabilities are expected in the absence of debris-related damage (i.e. a given flow depth may be deemed as more likely to cause damage if debris is also present in the flow). However, higher damage exceedance probabilities at higher TIM values are counterintuitive, and so the reason for this must be examined further.

Significance of Debris Parameter

A possible explanation for the removal of debris-damaged buildings from the dataset leading to increased damage exceedance probabilities at higher TIM values may be that this is simply due to the steepening of the curve (reduction in uncertainty or spread of the data, represented by the slope term, β_1) as a result of their being less data available (Table 2).

The significance of including debris data in the model can be investigated by forming a more complex model which includes a binary debris indicator variable, $debris_j$, indicating whether or not the building has been affected by debris (3) (i.e. $debris_j = 1$ for all buildings within grid squares which have a ratio of washed away footprint area to total area above the threshold percentage). The parameter $\beta_{2,i}$ in equation (3) adjusts the intercept of the model and equation (4) includes a fourth parameter $\beta_{2,i}$ which adjusts the slope of the model (an interaction term). In this way a single model can be formed which includes all engineered buildings and the significance of each parameter can be determined by their p-values (Table 4). A likelihood ratio test is then carried out to determine whether there is a significant increase in model accuracy with the addition of the debris terms (Table 5).

$$probit \left(P(ds \geq DS_i | TIM = x_j) \right) = \beta_{0,i} + \beta_{1,i} x_{j,k} + \beta_{2,i} debris_j \quad (3)$$

$$probit \left(P(ds \geq DS_i | TIM = x_j) \right) = \beta_{0,i} + \beta_{1,i} x_{j,k} + \beta_{2,i} debris_j + \beta_{3,i} x_{j,k} debris_j \quad (4)$$

The p-values in Table 4 show that all debris parameters are significant and that null hypothesis (that debris has no influence on damage state) can be rejected with the exception of the debris and debris interaction terms for DS1 ($\beta_{2,DS1}$ and $\beta_{3,DS1}$). The LRT results in Table 5 give p-values $\ll 0.001$ showing that the reduction in the residual sum of squares for the more complex model is statistically significant, so inclusion of debris improves the performance of fragility functions.

		Estimate	Std. Error	p	Significance
β_0	0 1.(Intercept)	2.44	0.08	1.14E-189	***
	1 2.(Intercept)	1.20	0.03	5.01E-294	***
	2 3.(Intercept)	0.11	0.03	2.89E-05	***
	3 4.(Intercept)	-1.41	0.05	1.31E-190	***
	4 5.(Intercept)	-1.45	0.05	2.93E-163	***
β_1	0 1 . $\ln h_{obsj} $	0.08	0.01	2.69E-31	***
	1 2 . $\ln h_{obsj} $	0.09	0.01	3.38E-52	***
	2 3 . $\ln h_{obsj} $	0.46	0.02	1.62E-124	***
	3 4 . $\ln h_{obsj} $	1.38	0.04	3.71E-296	***
	4 5 . $\ln h_{obsj} $	1.03	0.04	1.72E-119	***
β_2	0 1 . <i>debris_j</i>	0.13	0.21	5.36E-01	
	1 2 . <i>debris_j</i>	1.06	0.15	2.83E-12	***
	2 3 . <i>debris_j</i>	1.67	0.10	1.57E-64	***
	3 4 . <i>debris_j</i>	1.58	0.12	2.90E-38	***
	4 5 . <i>debris_j</i>	0.89	0.11	2.37E-15	***
β_3	0 1 . $\ln h_{obsj} $. <i>debris_j</i>	0.04	0.02	1.62E-02	*
	1 2 . $\ln h_{obsj} $. <i>debris_j</i>	0.91	0.23	6.58E-05	***
	2 3 . $\ln h_{obsj} $. <i>debris_j</i>	-0.24	0.04	1.74E-08	***
	3 4 . $\ln h_{obsj} $. <i>debris_j</i>	-0.61	0.08	1.44E-15	***
	4 5 . $\ln h_{obsj} $. <i>debris_j</i>	-0.46	0.07	6.89E-11	***

Table 4: Parameters of model (4). Significance codes are: *** = $p < 0.001$, ** = $p < 0.01$, * = $p < 0.05$.

Model Number	no.par	AIC	logLik	LR.stat	df	Pr(>Chisq)
(1)	10	11177.14	-5578			
(3)	15	10546.54	-5258	640.5995	5	<2.2e-16 ***
(4)	20	10399.99	-5180	156.5459	5	<2.2e-16 ***

Table 5: Likelihood ratio test results comparing models of increasing complexity based on observed inundation depth.

SUMMARY AND CONCLUSION

This paper has presented a preliminary methodology for quantifying debris-related effects on fragility functions. Detailed, disaggregated building-by-building damage data from the 2011 Great East Japan Earthquake (GEJE) has been used to develop tsunami fragility curves for engineered buildings in Japan for observed inundation depth and simulated force, considering the presence of debris in the flow. A 500m grid is applied to three case-study locations and buildings of each grid are deemed to have been affected by debris if the ratio of “washed away” building area to total building area within that grid exceeds a threshold proportion. Exploratory analysis was conducted of the total dataset of all buildings of engineered construction material (RC or steel) and of the debris-affected datasets. Fragility functions formed for all engineered buildings, and those deemed not to be affected by debris were compared, so that the effect of removing debris-damaged buildings from the regression dataset could be seen. More complex regression models were then formed incorporating a debris indicator variable (denoted 1 for all buildings considered to be affected by debris, and 0 for all other buildings) and an interaction term, so that the statistical significance of the debris parameters for each damage state could be examined. Finally, the models with and without debris parameters were compared using likelihood ratio tests so as to determine whether the inclusion of debris indicators in the model gave a significant improvement in the model fit.

The main results from this preliminary work are as follows:

- Buildings thought to be affected by debris mostly experienced higher TIM values and higher damage states (debris designation occurs in the vicinity of other ‘washed away’ buildings, which as more likely to occur in locations of high TIM values).
- The removal of buildings thought to be affected by debris resulted in changes to both the slope and intercept of the fragility functions. This indicates that the inclusion of debris-damaged buildings in the dataset (as is the case for most existing empirical fragility functions) does have an effect on fragility functions that may not be captured by purely flow regime-related TIMs.
- The difference between the intercept and slope (in link space) for fluid-only and debris-influenced fragility functions can be quantified by inclusion of debris-indicator terms in the fragility functions.
- The influence of debris model parameters on determining building damage was shown to be significant for all but the lowest damage state (“minor damage”).
- More complex fragility functions which incorporate debris model parameters were shown to have a statistically significant better fit to the observed damage data than models which omitted debris information. This suggests that inclusion of debris information in fragility functions improves the accuracy of the model.

Note that the method of identifying debris-damaged buildings in a dataset impact has not been the focus of this paper. The use of a grid, the grid size (500m) and the collapse area thresholds (50%, 35% and 20%) have all been subjective, and selected in order to allow the demonstration of the proposed methodology for quantifying debris effects on fragility function derivation. The optimal method of identifying and quantifying debris impact is the subject of further study, and along with the preliminary findings of this paper, will contribute to defining how fragility curves can be adjusted to account for increased damage probabilities in locations of increased likelihood of debris.

REFERENCES

- Adriano, B., & Koshimura, S. (2016). Understanding the extreme tsunami inundation in onagawa town by the 2011 tohoku earthquake, its effects in urban structures and coastal facilities. *Coastal Engineering Journal*.
- Charvet, I., Ioannou, I., Rossetto, T., Suppasri, a., & Imamura, F. (2014a). Empirical fragility assessment of buildings affected by the 2011 Great East Japan tsunami using improved statistical models. *Natural Hazards*, 73(2), 951–973. doi:10.1007/s11069-014-1118-3
- Charvet, I., Ioannou, I., Rossetto, T., Suppasri, A., & Imamura, F. (2014b). Empirical fragility assessment of buildings affected by the 2011 Great East Japan tsunami using improved statistical models. *Natural Hazards*. doi:10.1007/s11069-014-1118-3
- Charvet, I., Suppasri, A., Kimura, H., Sugawara, D., & Imamura, F. (2014). Fragility estimations for Kesenuma City following the 2011 Great East Japan Tsunami based on maximum flow depths, velocities and debris impact, with evaluation of the ordinal model’s predictive accuracy, 1–33.
- Imamura, F., Gica, E., Takahashi, T., & Shuto, N. (1995). Numerical Simulation of the 1992 Flores Tsunami: Interpretation of Tsunami Phenomena in Northeastern Flores Island and Damage at Babi Island. *Pure and Applied Geophysics*, 144, p555–568.
- Japan Cabinet Office. (2013). *Residential Disaster Damage Accreditation Criteria Operational Guideline.pdf*. Retrieved from <http://www.bousai.go.jp/taisaku/unyou.html>
- Lloyd, T. O. (2014). University College London An experimental investigation of tsunami forces on coastal structures.
- Macabuag, J., Rossetto, T., Ioannou, I., Suppasri, A., Sugawara, D., Adriano, B., ... Koshimura, S. (2016). Investigation of Optimum Intensity Measures and Advanced Statistical Methods for Constructing Tsunami Fragility Curves for Buildings. *Natural Hazards*, (tbc).
- Qi, Z. X., Eames, I., & Johnson, E. R. (2014). Force acting on a square cylinder fixed in a free-surface channel flow. *Journal of Fluid Mechanics*, 756, 716–727. doi:10.1017/jfm.2014.455
- Rossetto, T., Ioannou, I., Grant, D. N., & Maqsood, T. (2014). *Guidelines for Empirical Vulnerability Assessment Report produced in the context of the Vulnerability Global Component project*. Retrieved from <http://www.nexus.globalquakemodel.org/gem-vulnerability/posts/guidelines-for-empirical-vulnerability-assessment>

- Satake, K., Fujii, Y., Harada, T., & Namegaya, Y. (2013). Time and Space Distribution of Coseismic Slip of the 2011 Tohoku Earthquake as Inferred from Tsunami Waveform Data. *Bulletin of the Seismological Society of America*, *103*(2B), 1473–1492. doi:10.1785/0120120122
- Suppasri, A., Charvet, I., Kentaro, I., & Imamura, F. (2014). Fragility curves based on data from the 2011 Great East Japan tsunami in Ishinomaki city with discussion of parameters influencing building damage. *Earthquake Spectra*, *31*(2), 841–868. Retrieved from <http://earthquakespectra.org/doi/pdf/10.1193/053013EQS138M>
- Suppasri, A., Mas, E., Charvet, I., Gunasekera, R., Imai, K., Fukutani, Y., ... Imamura, F. (2013). Building damage characteristics based on surveyed data and fragility curves of the 2011 Great East Japan tsunami. *Natural Hazards*, *66*(2), 319–341. doi:10.1007/s11069-012-0487-8
- Suppasri, A., Mas, E., Koshimura, S., Imai, K., Harada, K., & Imamura, F. (2012). Developing Tsunami Fragility Curves From the Surveyed Data of the 2011 Great East Japan Tsunami in Sendai and Ishinomaki Plains. *Coastal Engineering Journal*, *54*(01), 1250008–1. doi:10.1142/S0578563412500088
- Tanaka, N., & Kondo, K. (2015). Fragility curve of region of wooden building washout due to tsunami based on hydrodynamic characteristics of the Great East Japan Tsunami. *Ocean Engineering*.